

Am Chem Soc. Author manuscript; available in PMC 2012 May 17.

Published in final edited form as:

JAm Chem Soc. 2010 December 15; 132(49): 17471–17482. doi:10.1021/ja108106h.

Advancing the Mechanistic Understanding of an Enantioselective Palladium-Catalyzed Alkene Difunctionalization Reaction

Katrina H. Jensena, Jonathan D. Webbb, and Matthew S. Sigmana,*

^aDepartment of Chemistry, University of Utah, 315 South 1400 East, Salt Lake City, Utah 84112

^bDepartment of Chemistry, Queen's University, 90 Bader Lane, Kingston, Ontario, Canada K7L 3N6

Abstract

The mechanism of an enantioselective palladium-catalyzed alkene difunctionalization reaction has been investigated. Kinetic analysis provides evidence of turnover limiting attack of a proposed quinone methide intermediate with MeOH and suggests that Cu is involved in productive product formation, not just catalyst turnover. Through examination of substrate electronic effects, a Jaffé relationship was observed correlating rate to electronic perturbation at two positions of the substrate. Ligand effects were evaluated to provide evidence of rapid ligand exchange between palladium and copper as well as a correlation between ligand electronic nature and enantioselectivity.

Introduction

Alkene difunctionalization, the formation of two new bonds from an alkene starting material, is a powerful synthetic method which rapidly increases molecular complexity.1–19 Such a transformation has the potential to set two new chiral centers, and thus methods to accomplish highly enantioselective and/or diastereoselective transformations catalytically are highly desirable. Palladium has become a popular metal of choice for alkene difunctionalization, likely due to its propensity to coordinate and activate alkene substrates for nucleophilic attack.3,4,20,21 However, due to facile β -hydride elimination from the resulting Pd(II)-alkyl intermediate, methods are required to prevent β -hydride elimination in order to allow for the second functionalization process. There are several classic strategies employed to circumvent this issue including using conjugated alkenes to form stabilized intermediates (such as π -allyl4,22–28 or π -benzyl complexes14,29) or trapping the Pd(II) intermediate by insertion of a second alkene.30–33 More recently, Pd(II)-alkyl intermediates have been oxidized to achieve alkene difunctionalization.10,11,34–41 While many of these approaches are highly diaseteroselective, few have been rendered enantioselective while also being able to introduce broad classes of nucleophiles.27,31,42–50

Recently, we reported the successful development of an enantioselective Pd-catalyzed alkene difunctionalization reaction wherein two distinct nucleophiles were added across an alkene in a stereo- and regioselective manner (Scheme 1).51 This reaction involves the use of substrates containing an alkene with an adjacent *ortho*-phenol and a linked nucleophile.

^{*}sigman@chem.utah.edu.

As has been discussed elsewhere and will be addressed in detail herein the $\it ortho$ -phenol is crucial;52 not only can it coordinate to the Pd(II)-intermediate preventing β -hydride elimination but it also is proposed to allow for the in situ formation of an electrophilic quinone methide species, necessary for the second functionalization to occur. Thus, our approach contrasts with others because oxidation of the substrate, not the Pd center, promotes the addition of the second nucleophile. The resulting reaction has broad scope as exogenous nucleophiles which form C-O, C-N, and C-C bonds have been successfully used in this chemistry.51,53 Furthermore, good to high enantioselectivity and diastereoselectivity are observed in most cases when a quinolineoxazoline chiral ligand (1) is employed. Copper salts were found to be essential additives to achieve effective catalysis without a detrimental effect on enantioselectivity when a sufficient amount chiral ligand is used. The ability to add two distinct nucleophiles across alkenes in a regio-, diastereo-, and enantioselective manner makes this contribution an important step in the advancement of alkene difunctionalization reactions. Therefore, in order to understand the precise details of this successful process, we have evaluated the mechanistic details which are presented herein.

Preliminary Mechanistic Hypothesis

We have previously reported the palladium-catalyzed dialkoxylation of alkenes with an adjacent *ortho*-phenol (Scheme 2). This work provided the initial evidence for the dual role of the *ortho*-phenol, preventing β -hydride elimination and allowing for the intermediacy of an *ortho*-quinone methide (Scheme 2, A).52 Support for these proposals include the requirement of an *ortho*-phenol in the alkene substrate as *para*-phenol substrates fail to provide product presumably due to their inability to prevent β -hydride elimination. Further, use of a protected phenol which should slow *ortho*-quinine methide formation, analogue 3, in the intermolecular alkene dialkoxylation reaction also did not result in product formation (Scheme 2, B). Additionally, when a deuterated substrate d_{4} -2 was submitted to the reaction no scrambling of the deuterium labels was observed, indicating that β -hydride elimination from **D** does not occur (Scheme 2, C).33

In general, quinone methides are considered to be reactive intermediates.54 They are inherently electrophilic because of the disruption to aromaticity; consequently, they react rapidly with most nucleophiles and dienophiles. The typical decomposition route for these species is homo dimer- or trimerization. Quinone methides can be stabilized by steric bulk54 or by coordination to electron rich transition metals complexes.55–58

(1)

An enantioselective variant of the dialkoxylation reaction was developed where it was found that the use of chiral quinoline oxazoline ligands provide products in high enantioselectivity (equation 1).45 Interestingly, a significant detrimental effect of added copper on enantioselectivity was observed (Table 1). Therefore, despite slightly diminished yields, the reaction was performed in the absence of copper. The limitations of this reaction were the use of the solvent as the nucleophile and the inability to add two distinct nucleophiles in a regioselective manner.

In contrast, in the development of the regioselective alkene difunctionalization reaction, it was found that copper was required for efficient catalysis.51 We hypothesized that the reason for the detrimental effect of copper on enantioselectivity was that copper and palladium compete for the chiral ligand, thus allowing for an achiral palladium species to catalyze the reaction, leading to nearly racemic product.45 In order to prevent this from occurring, copper and palladium complexes with (S)-quinox-IPr were prepared, making any ligand exchange inconsequential.51 Using 10 mol% Pd[(S)-quinox-IPr]Cl₂ and 20 mol% Cu[(S)-quinox-IPr]Cl₂ in the alkene difunctionalization reaction with substrate 5, product 6 was obtained with no decrease in enantioselectivity, but in substantially higher yield in a shorter reaction time (equation 2 vs. 3).

(2)

(3)

(4)

Further evidence in support of the proposed mechanism was provided by the isolation of 8, formed via a formal Diels-Alder reaction of propenyl ether 7 with the quinone methide intermediate under the standard alkene diffunctionalization conditions (equation 4).54 The major diastereomer is consistent with an inverse electron demand Diels-Alder reaction proceeding via an *endo* transition state with an *E*-quinone methide.54,59 The *E*-isomer of the quinone methide is assumed based on the steric interactions likely in the *Z*-isomer (Figure 1). The relative stereochemistry between the carbons α and β to the aromatic ring (originating from the alkene) matches that observed from the alkene dialkoxylation process, indicating that the dienophile approaches the quinone methide from the same face as an alcohol nucleophile.51 This facial selectivity is controlled either by the stereocenter on the tetrahydrofuran ring or potentially by the ligand on the metal(s), if bound.

When a lower *Z:E* ratio of propenyl ether **7** is used, the major diastereomer of **8** remains (*R,S,R,R*), but the relative amount of the diastereomer arising from the *E*-enol ether (*S,S,R,R*) increases (Table 2). Note that the ratio of (*R,S,R,R*) to (*S,R,S,R*), which arises from the facial selectivity in approach of the enol ether to the quinone methide, is nearly constant. These observations provide evidence for a concerted, albeit asynchronous, reaction, where the *E*-isomer of the enol ether reacts more slowly than the *Z*-isomer. Such a finding supports the existence of a quinone methide intermediate, as opposed to a stepwise mechanism involving insertion into the Pd-alkyl bond, followed by oxocarbenium formation, and attack by the phenol intermediate, as such a mechanism would not be expected to result in different diastereomers from each enol ether isomer.

We realize that the requirement of an alkene conjugated to an *ortho*-phenol is a limitation to this methodology, notwithstanding prospects for further functionalization. Nonetheless, we hypothesized that the proposed quinone methide intermediate could be utilized to develop other reactions, and therefore thought it would be beneficial to have a better understanding of the lifetime of this intermediate. Additionally, we suspected that the *ortho*-phenol may be influencing the stereochemical outcome of the reaction. Furthermore, the distinct effect of copper in this reaction pointed to the potential involvement of copper in steps other than simply palladium reoxidation.60 Given the widespread use of copper as a cocatalyst in palladium oxidase catalysis, we felt that evaluation of this possibility was warranted.31,61–63 We were interested in investigating the details of this transformation in order to develop a deeper understanding of the mechanism which will aid the future development of related palladium-catalyzed alkene difunctionalization reactions. Below we report mechanistic investigations undertaken, including kinetic analysis, evaluation of substrate electronic effects, and investigation of ligand perturbation on selectivity.

(5)

Kinetic Experiments

To probe both the lifetime of a proposed quinone methide intermediate and the role of copper in the reaction, a kinetic analysis was undertaken. The model substrate 5 was used with MeOH as the exogenous nucleophile (equation 5) to determine the dependence of reaction rate on various reaction components and the turnover limiting step of the reaction. Preformed complexes of Pd[(S)-quinox-IPr]Cl₂ and Cu[(S)-quinox-IPr]Cl₂ were used for all kinetic experiments for greater accuracy in weighing, as standard solutions could not be prepared at the desired concentrations due to low solubility. Note, however, that the solution becomes homogeneous upon addition of the substrate and remains homogeneous over the course of the reaction.

Kinetic measurements were obtained using an oxygen uptake instrument to monitor the rate of oxygen consumption (Figure 2, A).64 GC analysis was used to confirm that O_2 consumption corresponds to product yield, with 1/2 mmol O_2 consumed per mmol product formed. No O_2 consumption was observed in the absence of substrate. Further, when the reaction was performed under an N_2 atmosphere, no product was formed confirming the requirement of O_2 as an oxidant. Oxidation of MeOH to formaldehyde was not expected under the reaction conditions.52,65 Nevertheless, a control for this possibility was integrated into our experimental design: prior to each run the pressure was allowed to equilibrate over

the 4:1 toluene:MeOH solvent mixture containing catalysts and base (Figure 2, B). Once equilibrated O_2 consumption initiated immediately on addition of substrate (Figure 2, A and C). The small pressure increase during the equilibration period was the result of added vapor pressure from toluene and MeOH because of atmospheric cycling. A pseudo-order treatment of the O_2 data (Figure 2, C and D) did not provide a straight line across the reaction profile; however, there could be many reasons for this observation considering the complexity of this system. Nonetheless, the reaction was sufficiently well behaved up to ~50 % conversion to warrant initial rate analysis of the O_2 -uptake data. Initial rates were typically measured up to 5–10 % conversion based on O_2 consumption data and each plot contained more than 100 individual pressure measurements. This kinetic method was used to determine the dependence on the concentration of each component of the system.

First order dependence in [palladium] was observed (Figure 3), which points to a single palladium atom involved in catalysis. Saturation in [substrate] was observed (Figure 4, A), indicating that at low [substrate], substrate binding affects the overall rate of the reaction, but as [substrate] approaches a certain concentration palladium becomes saturated with substrate, and at this point increasing [substrate] does not increase reaction rate. This is consistent with substrate binding prior to the turnover limiting step. Nonetheless, many possibilities for the turnover limiting step remain, including nucleopalladation, quinone methide formation, attack of the quinone methide, and Pd⁰ oxidation.

Saturation in [Cu] was observed under conditions of substrate saturation (Figure 4, C), indicating a step prior to the turnover limiting step involves copper. This is evidence that copper is involved in a step other than just catalyst turnover. To determine if the saturation behavior in copper and substrate are independent, [substrate] and [Cu] dependence measurements were repeated at different conditions, such that [substrate] dependence was determined at both low and high [Cu] (Figure 4, A and B), and [Cu] dependence was determined at low and high [substrate] (Figure 4, C and D). It is interesting that in all four cases saturation is observed, suggesting that they are independent and thus occur in distinct steps. If both [copper] and [substrate] saturation occur in the same step, such as copper assisted substrate binding via the formation of a Cu-phenoxide (Figure 5), saturation behavior would depend on the total concentration of such a species ([substrate-Cu], equation 7), and thus [copper] and [substrate] saturation would not be independent.

$$K_{eq} = \frac{[\text{substrate} - \text{Cu}]}{[\text{substrate}][\text{Cu}]}$$
 (6)

[substrate-Cu] =
$$K_{eq}$$
 [substrate] [Cu] (7)

Concerned that some of these saturation effects might reflect a mass transport limited process, dependence on molecular oxygen uptake was evaluated by changing the partial pressure of O_2 and N_2 with a constant total system pressure. A zero order dependence in O_2 partial pressure was observed under conditions where the reaction was not saturated in [Cu]. This indicates that O_2 involvement in the reaction is subsequent to the turnover limiting step (Figure 6). The rate of reaction was also found to be independent of stir rate under these conditions (see Supporting Information). These observations coupled with the observation of a first order dependence in [catalyst] pointed to a reaction that was not mass transport limited in O_2 under low [Cu] conditions. This interpretation of mass transport effects in palladium catalyzed reactions is similar to that used by Steinhoff and Stahl in regard to aerobic alcohol oxidation.64 For these reasons low [Cu] conditions were considered to be kinetically well behaved and were used for subsequent reagent dependencies. It should be

noted that it is possible to observe modest mass transport effects at high concentrations of [Cu] and high total O_2 pressure (see Supporting Information).

The effect of base on reaction rate is complex (Figure 7). There appears to be a positive order in [KHCO₃] at low [KHCO₃] and inhibition at high [KHCO₃]. However, based on the observation that reaction yield also decreases as the [KHCO₃] is increased beyond 0.02 M, it is possible that this is a reflection of catalyst decomposition. In support of this conclusion, Pd-black precipitation is pronounced at higher base concentrations and O_2 uptake was negligible.

Finally, dependence on [MeOH] was determined at low [KHCO₃], where the reaction is well-behaved, and at high [substrate], where saturation is assumed. As discussed above this experiment was performed under conditions where the system was not saturated in [Cu] because increasing [MeOH] at high [substrate] and high [Cu] eventually results in a system that is limited by the rate of mass transport of molecular oxygen.66 A positive order in [MeOH] was observed (Figure 8, A). This suggests that MeOH is involved in the turnover limiting step. The relationship of ln(rate) vs. ln([MeOH]) has a slope less than one (0.66) (Figure 8, B), this is likely due to the fact that this experiment was performed under conditions where the system is not saturated in [Cu], which may result in a situation where more than one step is influencing the overall measured rate. While changing [MeOH] also has an effect on solution polarity, which may affect reaction rate, one would not expect to see a strong correlation from a polarity effect alone.

Dependence on [MeOH] also suggests that Pd is still bound when the quinone methide is attacked (Scheme 3, top), as attack by MeOH of a dissociated quinone methide (Scheme 3, bottom), even if rate limiting in terms of product formation, would allow palladium to reenter the catalytic cycle, and thus should not affect the rate of O_2 consumption. Additionally, if Pd was not bound, an accumulation of quinone methide in the reaction mixture would be expected and this was not observed.

With the kinetic data in hand, we needed to adjust our initially proposed mechanism to account for the observed kinetic results. Most significantly, our original mechanism needed to be modified to account for the observation of *independent* [Cu] and [substrate] saturation. In particular these results require a flexible pathway where turnover significant steps can change depending on the reaction conditions. Two distinct mechanisms involving copper in steps besides catalyst turnover or substrate binding were postulated (Scheme 4).67 The first three steps, which do not differ between the mechanisms, are the disassociation of an anionic ligand from intermediate A to provide an open coordination site on B, substrate binding to form C, and intramolecular nucleopalladation to reach Pd-alkyl species D. This portion of the mechanism invokes a substrate binding pathway which is similar to that observed in related systems68 and satisfactorily describes the observed saturation effect. In fact, K_1 for the interconversion of species of types **A** and **B** has been calculated from electrochemical studies when (-)-sparteine is the ligand.68,69 Note that bidentate substrate binding is assumed (vide infra), however, analogous mechanisms invoking monodentate substrate binding would also be consistent with the kinetic data. From the common intermediate **D**, the two proposed mechanisms differ. Recall that intermediate **D** is insufficiently electrophilic and incorrectly structured to account for the observed reactivity towards the nucleophiles and dienophiles. In mechanism A, D undergoes quinone methide formation via electron transfer from the electron rich organic framework to palladium.70 Copper is invoked as a Lewis acid to form the activated quinone methide species E, which undergoes nucleophilic attack by MeOH. Pd⁰ is oxidized to regenerate the active catalyst, a process most likely involving CuII, although direct O2 oxidation is possible in the absence of copper.45,71,72 In contrast, mechanism B accounts for the possibility of copper assisted

quinone methide formation. A possible redox mechanism to account for copper mediation involves coordination of copper to \mathbf{D} to form a hetero-bimetallic species \mathbf{H} , followed by oxidation to a Pd^{II} -quinone methide intermediate \mathbf{I} , likely through single electron transfer.73 Both mechanisms, account for a turnover limiting nucleophilic attack of the quinone methide intermediate by MeOH to form the product and release palladium when the system is saturated in [substrate] and/or [Cu]. It should be pointed out that the precise location of metals within a given intermediate cannot be deduced kinetically, and the structures merely represent a reasonable binding mode.

In mechanism A [Cu] operates as a Lewis acid; in mechanism B [Cu] has a redox role in the formation of the quinone methide. To determine if the role of [Cu] in the two mechanisms could be distinguished kinetically, a rate law was derived for each using the King-Altman method74 (Table 3, see SI for full derivation). Each derived rate law is rather complex. Therefore, to investigate whether each is consistent with empirical observations made under certain conditions, the rate laws were simplified by making assumptions specific to different sets of reaction conditions. In doing so, we observed that the simplified rate laws are relatively similar for both mechanisms, and are consistent with kinetic data. Specifically, when [Cu] is high, the simplified rate laws predict saturation in [substrate], as was observed. Likewise, when [substrate] is high, there is saturation in [Cu]. Finally, when both [substrate] and [Cu] are high, the rate laws reflect a first order dependence on [Pd_T] and [MeOH].

Neither of the proposed mechanisms can be ruled out as they are essentially indistinguishable kinetically, thus the specific role of copper remains ambiguous. We can, however, rule out a mechanism involving turnover limiting Pd⁰ to Pd^{II} oxidation by copper, as the rate law derived for this mechanism is inconsistent with empirically observed saturation in [Cu]. Furthermore, the proposal of turnover limiting attack of the quinone methide intermediate results in derived rate laws consistent with kinetic measurements.

Linear Free Energy Relationships

To probe the effect of substrate electronic perturbation on the reaction, a series of substrates with substitution at the 4-position were synthesized and evaluated. Initial rates were measured under conditions where saturation in [Cu] and [substrate] could be assumed in order to examine the proposed turnover limiting step. Because such a substitution has the potential to influence two reactive sites, either the phenol or the alkene, Hammett plots were constructed using both σ_p and σ_m values (Figure 9). Neither plot shows a linear correlation, suggesting electronic perturbation does not occur at just one site.

Considering the Hammett equation (Table 4), a Hammett plot should result in a linear relationship only if one position has a much more significant effect than the other (i.e. if $\sigma_m \gg \sigma_p$ or $\sigma_p \gg \sigma_m$). This is the case when a reactant has only one reactive site on an aromatic ring. However, in this reaction, both *meta* and *para* sites are potentially involved during the reaction. The Jaffé equation simply takes the Hammett equation and divides by one of the σ -values.75,76 This operation results in an equation which allows for a linear relationship even when two sites are perturbed. Depending on which σ -value is in the denominator, the slope of the resulting plot gives one ρ -value and the y-intercept gives the other ρ -value.

Two plots were constructed with the initial rate data measured in the alkene difunctionalization reaction (Figure 10). A linear free energy relationship is observed in both cases. The y-intercept from plot A is similar (within error) to the slope of plot B. This is crucial as both represent ρ_P . The same is true for ρ_{nn} , thus validating the linear free energy relationship.

Evaluation of the Jaffé plots reveals that $\rho_p \sim +2.3$ and $\rho_m \sim -1.2$. The resonance structure shown in Figure 11, which places a negative charge on the oxygen and a positive charge on the benzylic carbon, is often invoked to explain the reactivity of quinone methides.54 Such a species has a buildup of negative charge *para* to the R-substituent and positive charge *meta* to the R-substituent. If this species is involved in the transition state of the turnover limiting step, one would expect electron withdrawing groups to destabilize the positive charge at the *meta* position, leading to a negative ρ_m value. Likewise, electron donating groups *para* to the oxygen would destabilize the negative charge, and result in a positive ρ_p value. Thus the observed Jaffé relationship signifies a substituent effect consistent with turnover limiting quinone methide attack.

Probing the Role of Copper

Buoyed by the mechanistic insight gained from kinetic analysis, we were interested in exploring experiments to gain additional insight into the reaction mechanism in terms of the role of copper. If copper is acting as a Lewis acid, the ligand on copper may affect the selectivity of addition to the quinone methide intermediate. To probe this possibility, we chose to evaluate ligand effects on the diastereoselective outcome of the reaction. In order to perform such analysis, however, we needed to increase our understanding of ligand exchange. Based on the detrimental effect of unligated copper on enantioselectivity in the intermolecular alkene dialkoxylation reaction,45 we hypothesized that the ligand preferentially coordinates to copper, i.e. that the equilibrium of equation 8 lies to the right. If there is sufficient ligand, both metals are coordinated.

$$Pd[(S) - quinox - iPr]X_2 + CuX_2 \rightleftharpoons PdX_2 + Cu[(S) - quinox - iPr]X_2$$
 (8)

$$Pd(L) X2+Cu(L') X_2 \rightleftharpoons Pd(L') X_2+Cu(L) X_2$$
 (9)

However, if we start with preformed complexes of both metals, how rapid is ligand exchange between the two metals (eq. 9)? To answer this question, an experiment was designed wherein the palladium and copper complexes with opposite enantiomers of the ligand are employed in the reaction. A change in diastereoselectivity, either an increase or decrease, would indicate that copper is involved in the turnover limiting step and that the ligand on copper influences stereoinduction. A decrease in enantiomeric excess will indicate a loss of catalyst enantiopurity resulting from rapid ligand exchange. The use of Pd[(*R*)-quinox-*i*Pr]Cl₂ and Cu[(*S*)-quinox-*i*Pr]Cl₂ under the standard reaction conditions resulted in complete conversion to nearly racemic product (equation 10, 4% ee (*S*,*S*) and 7:1 dr, as compared to 93% ee (*R*,*R*) and 7:1 dr with Pd[(*S*)-quinox-*i*Pr]Cl₂ and Cu[(*S*)-quinox-*i*Pr]Cl₂). This points to rapid ligand exchange on the timescale of this reaction, thus no insight into ligand influence on diastereoselectivity was gained.

(10)

It was hypothesized that other ligands may not exchange as rapidly. Thus copper complexes with 2,2'-bipyridine, phenanthroline, and bathocuproine were prepared and evaluated (Table 5). Catalytic systems with Cu(bipyridine)Cl₂ (entry 1) and Cu(phenanthroline)Cl₂ (entry 2)

were significantly slower, with only 3% and 7% yields, respectively, at 30 min compared to complete conversion for the all-(S)-quinox-IPr system. Additionally, ligand exchange occurs between copper and palladium, as the enantiomeric excess of the product decreases as the reaction progresses (80% ee at 30 min and 12% ee at completion for Cu(bipyridine)Cl₂, entry 1 and 81% ee at 30 min and 18% ee at completion for Cu(phenanthroline)Cl₂, entry 2). Interestingly, Cu(bathocuproine)Cl₂ behaves differently (entry 3). The reaction is complete within 2 h, with good yield and only slightly diminished enantiomeric excess (91% ee), and a similar diastereomeric ratio (7:1) as observed with Cu[(S)-quinox-iPr]Cl₂ (93% ee and 7:1 dr). In contrast to the systems using Cu(bipyridine)Cl₂ and Cu(phenanthroline)Cl₂, ee is constant over the course of the reaction with Cu(bathocuproine)Cl₂, implying that ligand exchange does not occur. However, another explanation exists: ligand exchange is rapid, and the resulting Pd(bathocuproine) X_2 catalyst is significantly less active than the Pd[(S)quinox-iPr]X₂ catalyst. In exploring this possibility, a control experiment was performed using bathocuproine as the ligand for both metals (entry 4). This reaction is indeed significantly slower, with only 5% yield after 2 h, and 27% yield with near complete conversion of the substrate at 17 h. Unfortunately, given the potential for ligand exchange, no evidence was gained to either indicate or rule out copper involvement in the diastereoselective step. Nevertheless, a highly enantioselective system using an achiral ligand on copper was discovered, thus reducing the necessary loading of chiral material by more than half.

To further probe the possibility of copper acting as a simple Lewis acid, other Lewis acid additives were tested in the reaction (Table 6, see supporting information for complete list of Lewis acids evaluated). Of all of the Lewis acids tested, only FeCl₃ (entries 4 & 5) and ZnCl₂ (entries 6 & 7) demonstrated a positive effect on the product yield compared to the reaction without an added Lewis acid (entry 1). Even in these cases, however, the reaction is much slower, with completion occurring after approximately 24 h, whereas the reactions employing copper are complete in approximately 30 min (entries 2 and 3). While this does not rule out the possibility of copper acting as a Lewis acid to activate the quinone methide intermediate for attack, which would explain the positive effect with ZnCl₂, it suggests that it is likely serving another purpose as well. Copper is known to catalyze the oxidation of catechol to quinone with molecular oxygen,73 and a similar process could occur in this reaction. Moreover, the observation that FeCl₃ improves product yield, albeit at a significantly slower rate than copper, is in agreement with this analysis, as iron has also been shown to facilitate quinone formation.77 Therefore, mechanism B, where copper acts to facilitate quinone methide formation, is the favored mechanism.

Origin of Stereoselectivity

A better understanding of the origin of enantioselectivity would be beneficial for future reaction development. Our stereochemical analysis invokes initial nucleopalladation at the β -position as the enantiodetermining step. When considering the development of a stereochemical model for this reaction, many variables affecting selectivity on nucleopalladation need to be taken into account. Two possible mechanisms for this step are *cis*-nucleopalladation, where both the alkene and the nucleophile are coordinated to palladium, and the alkene inserts into the Pd-Nu bond, and *trans*-nucleopalladation, where the nucleophile attacks the alkene from the face opposite palladium. Unfortunately, because the stereochemical information at the α -position is lost upon quinone methide formation, it is difficult to envision a method to directly elucidate the precise mechanistic nature of this step. Furthermore, because this step is fast, it cannot be probed kinetically. If *trans*-nucleopalladation is operative, there is the potential for the substrate to be bound to palladium in either a monodentate or bidentate mode (through the alkene and the phenoxide). Further complicating the analysis, it cannot be determined whether the *E*- or *Z*-

isomer of the alkene is the reactive species, since alkene isomerization has been shown to be rapid.52 Additionally, because the ligand is not C_2 -symmetric, the two potential coordination sites are not identical. In light of these issues, we reasoned that the best way to probe the enantiodetermining nucleopalladation step is through a systematic examination of ligand effects.

While (S)-quinox-IPr was found to be the optimal chiral ligand for this reaction, it was observed that the reaction using (S)-pyrox-tBu is well behaved and gives relatively high enantiomeric excess (82%). It was presumed that derivatives of (S)-pyrox-tBu would be synthetically easier to access than those of (S)-quinox-IPr. Therefore, a series of 4substituted pyrox-tBu ligands was chosen for evaluation of ligand electronic effects. Ligands 17-21 were synthesized in two steps from commercially available picolinic acid derivatives (see SI for details), and tested in the Pd-catalyzed alkene difunctionalization reaction under our standard conditions. A subtle ligand electronic effect on enantioselectivity was revealed (Table 7). A linear free energy relationship was observed by plotting log(er) vs. Hammett σ values with $\rho = -0.34$ (Figure 12). A negative ρ value indicates that more electron rich ligands lead to improved enantioselectivity. However, it should be noted that the electron rich ligands have nearly the same enantiomeric ratio but their selectivity is better than that of electron withdrawing ligands. An unanticipated outcome of this set of experiments was an observed ligand modulated enhancement of the diastereoselectivity. This result supports the assertion that the ligated metal species is intimately involved in the addition of the exogenous nucleophile.

A reasonable explanation to account for this modest effect was postulated: a palladium alkene intermediate that is more electron rich is less electrophilic, and thus at a lower energy than the analogous system with an electron poor substituent on the ligand. This suggests that the nucleopalladation reaction is less exothermic, and thus by the Hammond postulate, goes through a later transition state. Such a transition state is more product-like, where there should be a greater difference between the activation energies to reach the two enantiomers.

Our stereochemical analysis invokes initial nucleopalladation at the β -position as the enantiodetermining step. Evidence for this hypothesis was provided when trisubstituted alkene **22** was submitted to the intermolecular alkene dialkoxylation reaction conditions.45 The product **23** was obtained in 0% ee (Scheme 5), indicative of initial oxypalladation at the β -position. As two of the substituents are at this position are identical, the subsequent quinone methide intermediate is achiral, leading to racemic product. A mechanism involving enantioselective addition at the α -position would be expected to result in enantiomerically enriched product **23**. Further, as previously reported, the nucleophile employed has an influence on diastereoselectivity generally leaving enantioselectivity unperturbed. Thus we make the assumption that a bidendate substrate-Pd species undergoes nucleopalladation, as reflected in proposed mechanisms A and B (Scheme 4). Nevertheless, mechanisms invoking monodendate substrate binding may be drawn.

Given the significant number of variables associated with nucleopalladation, several assumptions need to be made in order to develop a working stereochemical model. First, it is assumed that intramolecular nucleopalladation occurs on a Pd-substrate species which is bidentate, coordinated through the alkene and the phenoxide. Given the evidence that nucleophilic attack occurs at the anti-Markovnikov β -position, it seems necessary to invoke a reason for this normally electron-rich site to be the more electrophilic site upon coordination. Substrate binding in a bidentate fashion would require the aromatic ring to rotate out of conjugation with the alkene, and thus inhibit the phenol's ability to donate electron density to the alkene. This hypothesis is supported by the mixture of products

obtained with a protected phenol substrate **3** (Scheme 2, B).52 Furthermore, the modest substrate electronic effects on enantioselectivity (Table 8) is consistent with the alkene being out of conjugation with the aromatic ring during nucleopalladation. Interestingly, the diastereoselectivity is loosely related to electron donation to the phenol, this is in contrast to insensitivity observed when ligand electronics were modified (Table 7).

The assumption that a bidentate substrate-Pd species undergoes nucleopalladation eliminates the possibility of a cis-nucleopalladation pathway because all four coordination sites on the square plane of palladium are occupied. This leaves eight possible binding geometries to obtain the product (two possible alkene isomers, two possible faces of each alkene, two possible sites for the alkene to coordinate). The second assumption is that, given the bulky nature of the substituent on the oxazoline, the substrate will coordinate in a manner that orients the alkyl chain toward the opposite face of the palladium-plane. This eliminates four of the eight possibilities. Two of the remaining possibilities lead to the minor enantiomer of the product. The last two possibilities are (1) the E-isomer bound trans to the oxazoline, and (2) the Z-isomer bound trans to the pyridine. In examination of physical models, the former seems to have slight steric interactions between the alkyl chain and the pyridine portion of the ligand, while the latter seems to orient the chain away from the ligand. Also, the latter possibility orients the alkene closer in space to the chiral center on the ligand. Further, this orientation provides for the observed electronic communication between the ligand and substrate as described above. Finally, it would be difficult to envision how asymmetric induction could be imparted if the alkene was oriented away from the oxazoline. Thus, the model shown in Figure 13 is presented to explain the observed facial selectivity. While thermodynamically less stable than the E-isomer, the Z-alkene may be the more reactive species, both in terms of alkene binding and ability to access conformers that lead to product formation. Furthermore, a stereochemical model which involves coordination of the alkene trans to the pyridine is consistent with the observed electronic effect of the ligand on enantioselectivity.

Conclusion

Detailed investigation of a palladium-catalyzed alkene difunctionalization reaction provided insight into the mechanistic details. Kinetic evidence for turnover limiting attack of the quinone methide was uncovered, supported by the observation of a linear free energy relationship correlating substrate electronic nature to the rate of reaction. The Jaffé relationship is used to interpret the complex influence of an aromatic substituent when there are two potential reactive sites on the aromatic ring, providing further support for turnover limiting quinone methide attack. While the precise function of copper in this reaction was not elucidated, evidence for copper involvement in more than just catalyst turnover was discovered. The kinetic data and results using other Lewis acids support copper facilitated quinone methide formation. Ligand exchange between copper and palladium was found to be rapid in most cases, but an enantioselective system was developed which uses an achiral copper complex in conjunction with a chiral palladium complex, thus reducing the loading of chiral material. Finally, we hope to take advantage of these findings to design new alkene functionalization manifolds in which the substrate undergoes oxidation to a reactive intermediate.

Supplementary Material

Refer to Web version on PubMed Central for supplementary material.

Acknowledgments

This work was supported by the National Institute of Health (NIGMS RO1 GM3540). M.S.S. thanks the Dreyfus Foundation (Teacher-Scholar) and Pfizer for their support. J.D.W. is grateful for the award of a Queen's University Dean's Travel Grant. We are grateful to Johnson Matthey for the gift of various Pd-salts.

REFERENCES

- (1). Kolb HC, VanNieuwenhze MS, Sharpless KB. Chem. Rev. 1994; 94:2483.
- (2). Cardona F, Goti A. Nat. Chem. 2009; 1:269. [PubMed: 21378869]
- (3). Jensen KH, Sigman MS. Org. Biomol. Chem. 2008; 6:4083. [PubMed: 18972034]
- (4). Bäckvall J-E. Met.-Catal. Cross-Coupling React (2nd Ed.). 2004; 2:479.
- (5). Benkovics T, Du J, Guzei IA, Yoon TP. J. Org. Chem. 2009; 74:5545. [PubMed: 19507883]
- (6). Paderes MC, Chemler SR. Org. Lett. 2009; 11:1915. [PubMed: 19331361]
- (7). Baeckvall JE, Nordberg RE. J. Am. Chem. Soc. 1981; 103:4959.
- (8). Zabawa TP, Kasi D, Chemler SR. J. Am. Chem. Soc. 2005; 127:11250. [PubMed: 16089447]
- (9). Zeng W, Chemler SR. J. Am. Chem. Soc. 2007; 129:12948. [PubMed: 17918850]
- (10). Kalyani D, Sanford MS. J. Am. Chem. Soc. 2008; 130:2150. [PubMed: 18229926]
- (11). Wang A, Jiang H, Chen H. J. Am. Chem. Soc. 2009; 131:3846. [PubMed: 19292485]
- (12). Rosewall CF, Sibbald PA, Liskin DV, Michael FE. J. Am. Chem. Soc. 2009; 131:9488. [PubMed: 19545153]
- (13). Rodriguez A, Moran WJ. Eur. J. Org. Chem. 2009:1313.
- (14). Urkalan KB, Sigman MS. Angew. Chem., Int. Ed. 2009; 48:3146.
- (15). Tsujihara T, Takenaka K, Onitsuka K, Hatanaka M, Sasai H. J. Am. Chem. Soc. 2009; 131:3452. [PubMed: 19275254]
- (16). Chevrin C, Le Bras J, Henin F, Muzart J. Synthesis. 2005:2615.
- (17). Thiery E, Chevrin C, Le Bras J, Harakat D, Muzart J. J. Org. Chem. 2007; 72:1859. [PubMed: 17274660]
- (18). Demko ZP, Bartsch M, Sharpless KB. Org. Lett. 2000; 2:2221. [PubMed: 10930248]
- (19). Fuller PH, Kim J-W, Chemler SR. J. Am. Chem. Soc. 2008; 130:17638. [PubMed: 19049311]
- (20). Semmelhack MF, Bodurow C. J. Am. Chem. Soc. 1984; 106:1496.
- (21). Beccalli EM, Broggini G, Martinelli M, Sottocornola S. Chem. Rev. 2007; 107:5318. [PubMed: 17973536]
- (22). Bäckvall JE, Bystroem SE, Nordberg RE. J. Org. Chem. 1984; 49:4619.
- (23). Bäckvall JE, Nystroem JE, Nordberg RE. J. Am. Chem. Soc. 1985; 107:3676.
- (24). Bäckvall JE, Vaagberg JO. J. Org. Chem. 1988; 53:5695.
- (25). Bar GLJ, Lloyd-Jones GC, Booker-Milburn KI. J. Am. Chem. Soc. 2005; 127:7308. [PubMed: 15898768]
- (26). Du H, Yuan W, Zhao B, Shi Y. J. Am. Chem. Soc. 2007; 129:7496. [PubMed: 17521192]
- (27). Du H, Zhao B, Shi Y. J. Am. Chem. Soc. 2008; 130:8590. [PubMed: 18549207]
- (28). Zhao B, Du H, Cui S, Shi Y. J. Am. Chem. Soc. 2010; 132:3523. [PubMed: 20166669]
- (29). Werner EW, Urkalan KB, Sigman MS. Org. Lett. 2010; 12:2848. [PubMed: 20481606]
- (30). Scarborough CC, Stahl SS. Org. Lett. 2006; 8:3251. [PubMed: 16836378]
- (31). Kawamura Y, Kawano Y, Matsuda T, Ishitobi Y, Hosokawa T. J. Org. Chem. 2009; 74:3048. [PubMed: 19296642]
- (32). Kawamura Y, Imai T, Hosokawa T. Synlett. 2006:3110.
- (33). Minami K, Kawamura Y, Koga K, Hosokawa T. Org. Lett. 2005; 7:5689. [PubMed: 16321023]
- (34). Liu G, Stahl SS. J. Am. Chem. Soc. 2006; 128:7179. [PubMed: 16734468]
- (35). Alexanian EJ, Lee C, Sorensen EJ. J. Am. Chem. Soc. 2005; 127:7690. [PubMed: 15913354]
- (36). Desai LV, Sanford MS. Angew. Chem., Int. Ed. 2007; 46:5737.

(37). Welbes LL, Lyons TW, Cychosz KA, Sanford MS. J. Am. Chem. Soc. 2007; 129:5836. [PubMed: 17432861]

- (38). Streuff J, Hoevelmann CH, Nieger M, Muniz K. J. Am. Chem. Soc. 2005; 127:14586. [PubMed: 16231907]
- (39). Qiu S, Xu T, Zhou J, Guo Y, Liu G. J. Am. Chem. Soc. 2010; 132:2856. [PubMed: 20148557]
- (40). Li Y, Song D, Dong VM. J. Am. Chem. Soc. 2008; 130:2962. [PubMed: 18281992]
- (41). Park CP, Lee JH, Yoo KS, Jung KW. Org. Lett. 2010; 12:2450. [PubMed: 20455553]
- (42). Xu L, Shi Y. J. Org. Chem. 2008; 73:749. [PubMed: 18095707]
- (43). Arai MA, Kuraishi M, Arai T, Sasai H. J. Am. Chem. Soc. 2001; 123:2907. [PubMed: 11456988]
- (44). Yip K-T, Yang M, Law K-L, Zhu N-Y, Yang D. J. Am. Chem. Soc. 2006; 128:3130. [PubMed: 16522078]
- (45). Zhang Y, Sigman MS. J. Am. Chem. Soc. 2007; 129:3076. [PubMed: 17298071]
- (46). He W, Yip K-T, Zhu N-Y, Yang D. Org. Lett. 2009; 11:5626. [PubMed: 19905004]
- (47). Aratani T, Tahara K, Takeuchi S, Ukaji Y, Inomata K. Chem. Lett. 2007; 36:1328.
- (48). Shinohara T, Arai MA, Wakita K, Arai T, Sasai H. Tetrahedron Lett. 2003; 44:711.
- (49). Sperrle M, Consiglio G. J. Mol. Catal. A: Chem. 1999; 143:263.
- (50). Wang C, Tunge JA. J. Am. Chem. Soc. 2008; 130:8118. [PubMed: 18533718]
- (51). Jensen KH, Pathak TP, Zhang Y, Sigman MS. J. Am. Chem. Soc. 2009; 131:17074. [PubMed: 19902942]
- (52). Schultz MJ, Sigman MS. J. Am. Chem. Soc. 2006; 128:1460. [PubMed: 16448111]
- (53). Pathak TP, Gligorich KM, Welm BE, Sigman MS. J. Am. Chem. Soc. 2010; 132:7870. [PubMed: 20486685]
- (54). Van De Water RW, Pettus TRR. Tetrahedron. 2002; 58:5367. [PubMed: 19079773]
- (55). Vigalok A, Milstein D. Acc. Chem. Res. 2001; 34:798. [PubMed: 11601964]
- (56). Amouri H, Le Bras J. Acc. Chem. Res. 2002; 35:501. [PubMed: 12118989]
- (57). Stokes SM, Ding F, Smith PL, Keane JM, Kopach ME, Jervis R, Sabat M, Harman WD. Organometallics. 2003; 22:4170.
- (58). Poverenov E, Shimon LJW, Milstein D. Organometallics. 2007; 26:2178.
- (59). Arduini A, Bosi A, Pochini A, Ungaro R. Tetrahedron. 1985; 41:3095.
- (60). Tsuji, J. Palladium Reagents and Catalysts: New Perspectives for the 21st Century. John Wiley & Sons; New York: 2004. Oxidative Reactions with Pd(II) Compounds; p. 27
- (61). Takacs JM, Jiang X.-t. Curr. Org. Chem. 2003; 7:369.
- (62). Hosokawa T, Takano M, Murahashi S-I. J. Am. Chem. Soc. 1996; 118:3990.
- (63). Hosokawa T, Nomura T, Murahashi S-I. J. Organomet. Chem. 1998; 551:387.
- (64). Steinhoff BA, Stahl SS. J. Am. Chem. Soc. 2006; 128:4348. [PubMed: 16569011]
- (65). Gligorich KM, Schultz MJ, Sigman MS. J. Am. Chem. Soc. 2006; 128:2794. [PubMed: 16506746]
- (66). A dependence on stir rate was observed at high [Cu], indicative of a system that is limited my mass transport of oxygen. See Supporting Information for details.
- (67). Catalyst saturation can imply reversible formation of higher order metal complexes in situ. However, such saturation curves are often marked by large x-intercepts and/or pronounced slopes reflective of the binding constants which are not observed here.
- (68). Anderson BJ, Keith JA, Sigman MS. J. Am. Chem. Soc. 2010; 132:11872. [PubMed: 20687555]
- (69). Mueller JA, Cowell A, Chandler BD, Sigman MS. J. Am. Chem. Soc. 2005; 127:14817. [PubMed: 16231935]
- (70). Alternatively, D and E could be interpreted as resonance structures. However, it is unclear whether Pd remains coordinated to both the oxygen atom and the benzylic carbon in the Pd-quinone methide intermediate. Therefore, we have chosen to depict D and E as distinct intermediates to allow for the possibility of atom movement. These two interpretations result in the same derived rate law.
- (71). Sigman MS, Jensen DR. Acc. Chem. Res. 2006; 39:221. [PubMed: 16548511]

(72). Stahl SS. Angewandte Chemie International Edition. 2004; 43:3400.

- (73). Balla J, Kiss T, Jameson RF. Inorg. Chem. 1992; 31:58.
- (74). King EL, Altman C. J. Phys. Chem. 1956; 60:1375.
- (75). Jaffe HH. J. Am. Chem. Soc. 1954; 76:4261.
- (76). Edwards DR, Neverov AA, Brown RS. J. Am. Chem. Soc. 2009; 131:368. [PubMed: 19055404]
- (77). Smith LI, Davis HR Jr. Sogn AW. J. Am. Chem. Soc. 1950; 72:3651.
- (78). Palucki M, Finney NS, Pospisil PJ, Gueler ML, Ishida T, Jacobsen EN. J. Am. Chem. Soc. 1998; 120:948.

Figure 1. Stereochemical model for diastereoselectivity.

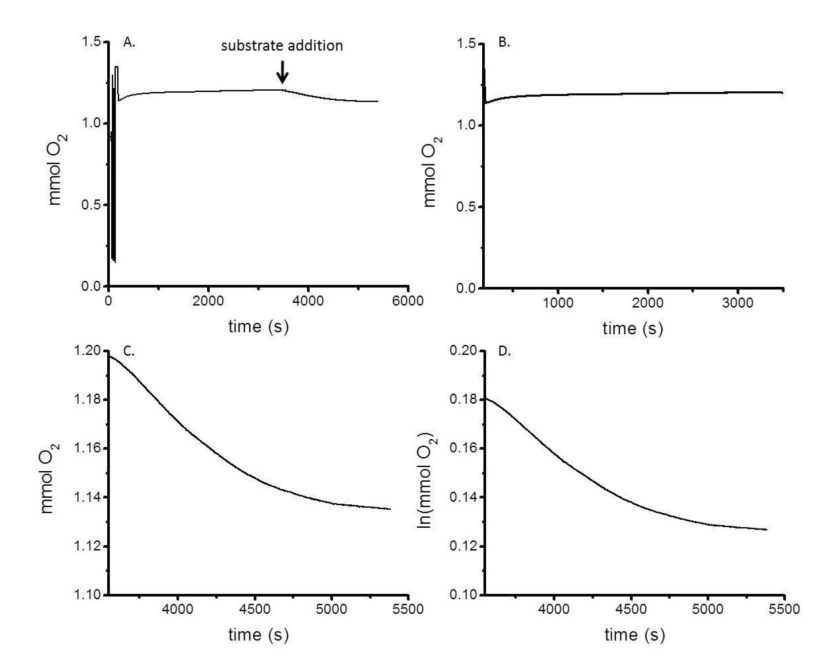


Figure 2.Typical reaction profiles as measured by O₂ uptake. A. Full O₂ uptake profile. B. Equilibration time. C. Pseudo-zero order reaction profile. D. Pseudo-first order reaction profile.

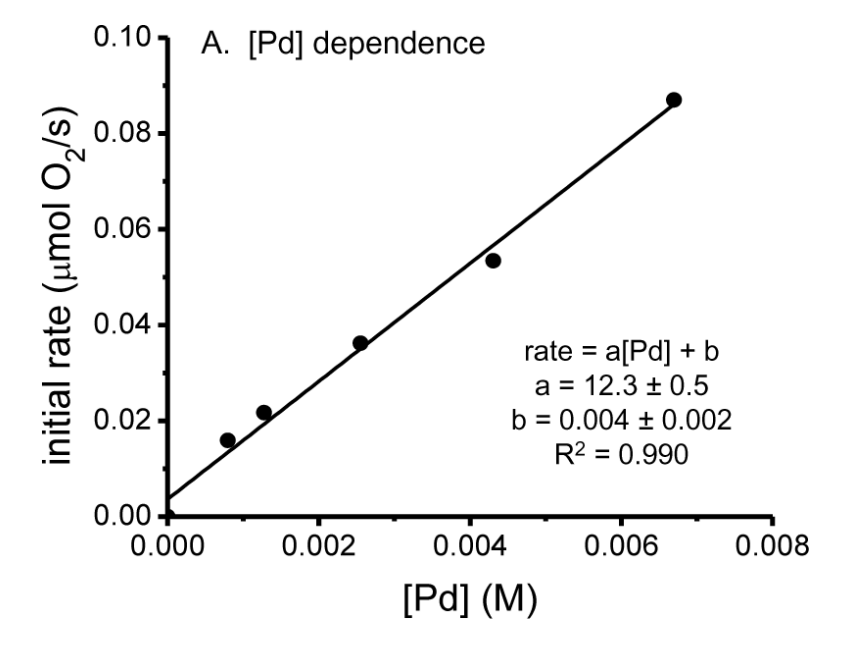


Figure 3. First order dependence on [Pd]. Conditions: [substrate] = 0.16 M, [Cu] = 0.0017 M [KHCO₃] = 0.026 M, 1:4 MeOH:toluene, O_2 , 25 °C.

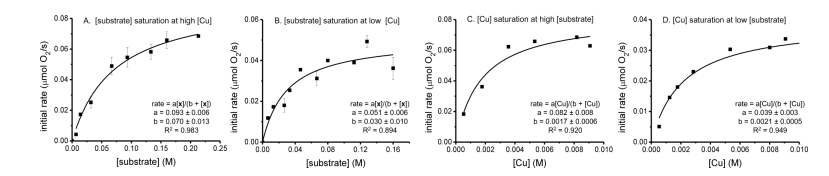


Figure 4. Saturation in [substrate] and [Cu]. Conditions: [Pd] = 0.0026 M, [KHCO₃] = 0.026 M, 1:4 MeOH:toluene, O₂, 25 °C, A. [Cu] = 0.0053 M, B. [Cu] = 0.0017 M, C. [substrate] = 0.16 M, D. [substrate] = 0.026 M

$$\begin{array}{c} \text{OH} \\ \text{OH} \\ \text{OH} \\ \text{OH} \end{array} + \begin{array}{c} \text{CuX}_2 \\ \text{OH} \\ \text{OH} \\ \text{OH} \end{array} + \begin{array}{c} \text{HX} \\ \text{OH} \\ \text{OH}$$

Figure 5. Formation of substrate-copper complex. Does not account for observed independent saturation in [substrate] and [Cu].

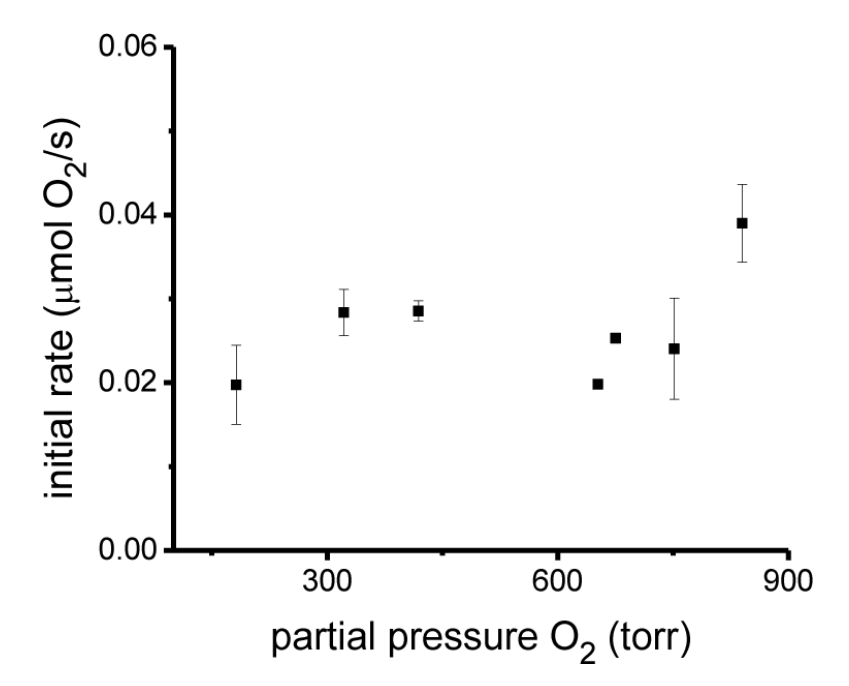


Figure 6. Zero order dependence on partial pressure of O_2 (with N_2), conditions: [Pd] = 0.0026 M, [Cu] = 0.0017 M, [substrate] = 0.16 M, [KHCO₃] = 0.026 M, 1:4 MeOH:toluene, 25 °C, total pressure = 850 torr.

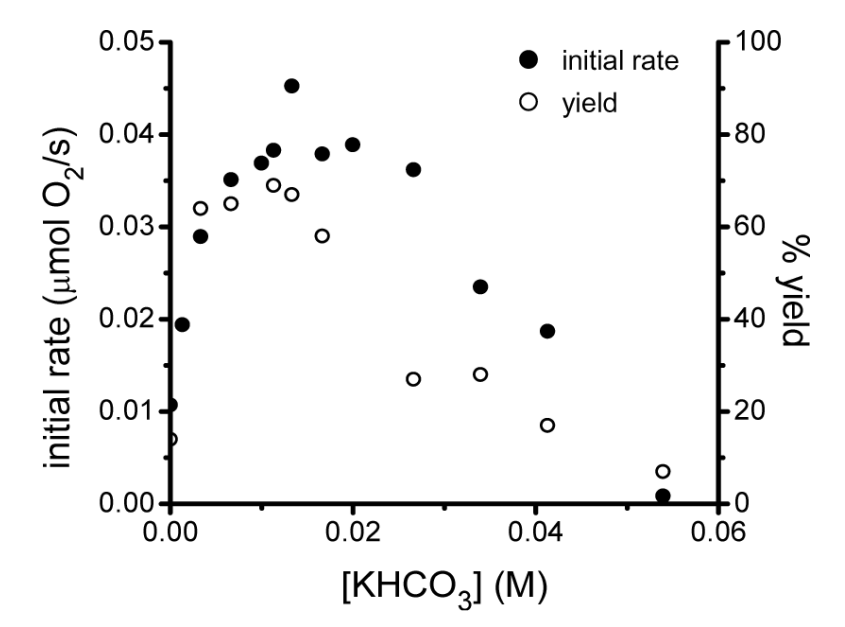


Figure 7. Dependence of rate and yield on [KHCO₃], conditions: [Pd] = 0.0026 M, [Cu] = 0.0017 M, [substrate] = 0.16 M, 1:4 MeOH:toluene, O₂, 25 °C.

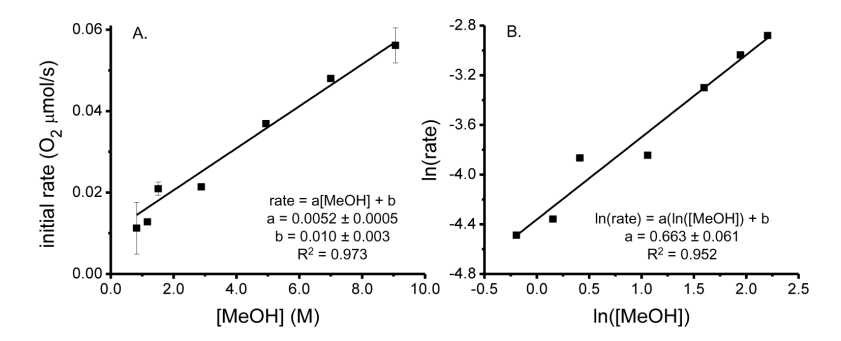


Figure 8. Positive dependence on [MeOH], conditions: [Pd] = 0.0026 M, [Cu] = 0.0017 M, [substrate] = 0.16 M, [KHCO₃] = 0.010 M, O_2 , 25 °C.

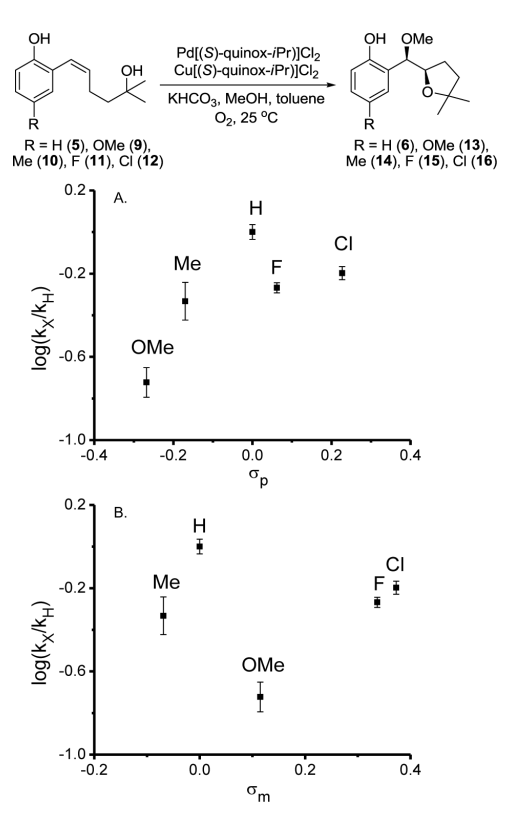


Figure 9. Evaluation of substrate electronic effect on rate. Hammett plots: $\log(k_X/k_H)$ vs. $\sigma_p(A)$ and $\sigma_m(B)$.

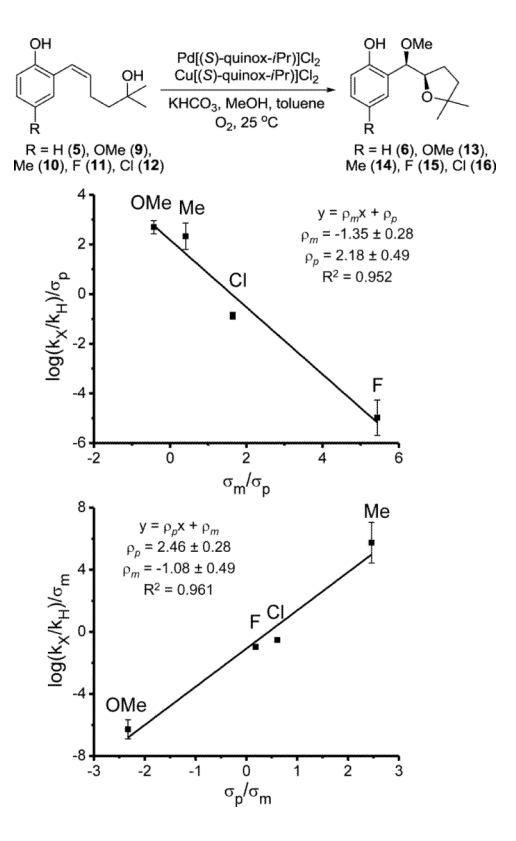


Figure 10. Jaffé plots show a linear free energy relationship between substrate electronics and reaction rate. ρ_D and ρ_m values from each plot are within error.

Figure 11. Quinone methide resonance structures.

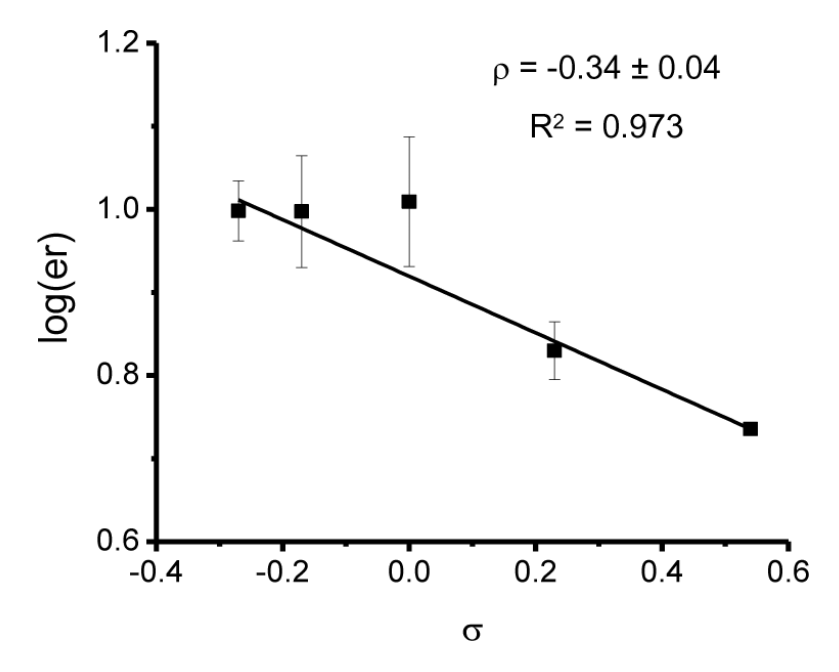


Figure 12. Hammett plot of $\log(er)$ vs. σ showing ligand electronic effect on enantioselectivity.

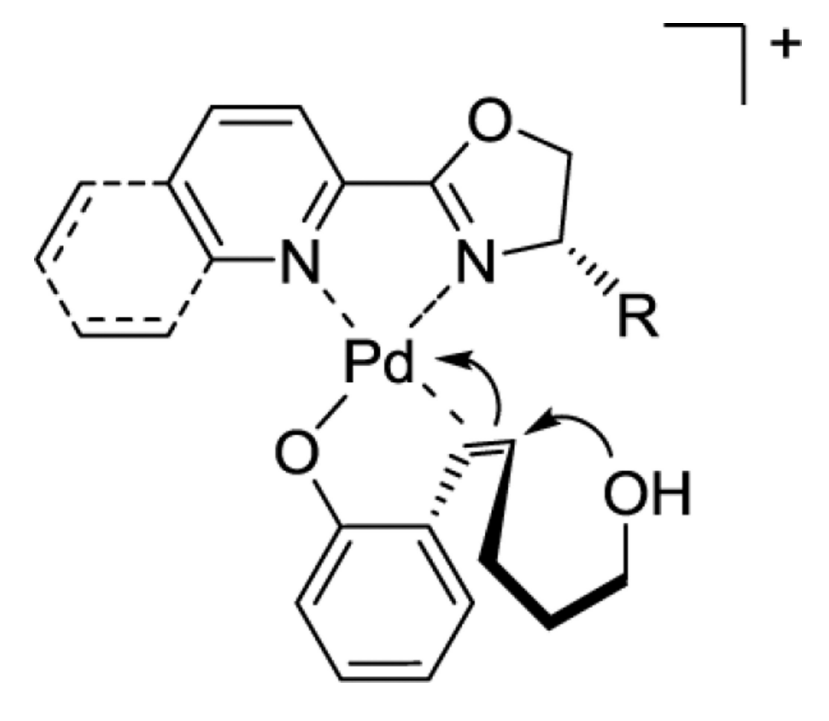


Figure 13. Working stereochemical model.

Scheme 1.

Pd-catalyzed difunctionalization of alkenes with an adjacent *ortho*-phenol and tethered nucleophile.

Scheme 2. Initial discovery of Pd-catalyzed alkene dialkoxylation and evidence for a quinone methide intermediate.

Scheme 3. Evidence for attack of palladium-bound quinone methide intermediate.

Scheme 4. Proposed mechanisms to account for potential role of copper.

Scheme 5. Evidence for initial oxypalladation at the β -position.

Table 1

Detrimental effect of copper on enantioselectivity in Pd-catalyzed alkene dialkoxylationw $_{OH}^{OH}$ $_{10 \text{ mol}\%}$ $_{Pd(MeCN)_2Cl_2}^{OH}$ $_{OMe}^{OH}$ $_{OMe}^{OH}$

moI% CuCI ₂	% GC yield	% ee	er
0	67	82	91:9
2.5	80	72	86:14
5	78	59	80:20
10	81	26	63:37
20	88	10	55:45

Table 2

Jensen et al.

Effect of enol ether isomeric ratio on diastereoselectivity.

OEt H O S. S. R., R.)-8		0.3	0.5	1.4
+				
, OEt H H D O O O O O O O O O O O O O O O O O		1	1	1
H. R. B8				
OEt H O.S.R.R.)-8		7.1	8.5	8.7
200	Z:E	1	1	1
// _	' '	10:1	4.8:1	1.6:1

Page 34

Table 3

Derived and simplified rate laws for proposed mechanisms.

Derived Rate Laws

Mechanism A

$$\frac{\text{d[P]}}{\text{dt}} = \frac{1}{\left(k_{2}k_{3}k_{4}k_{5}k_{6}[\text{sub}][\text{Cu}][\text{MeOH}][\text{Ox}][\text{base}]^{2} + k_{-1}k_{3}k_{4}k_{5}k_{6}[\text{Cu}][\text{MeOH}][\text{X}^{-}][\text{Ox}][\text{base}] + k_{-1}k_{-2}k_{4}k_{5}k_{6}[\text{Cu}][\text{MeOH}][\text{X}^{-}]^{2}[\text{Ox}] + k_{1}k_{3}k_{4}k_{5}k_{6}[\text{Cu}][\text{MeOH}][\text{X}^{-}]^{2}[\text{Ox}] + k_{1}k_{3}k_{4}k_{5}k_{6}[\text{Cu}][\text{N}^{-}]^{2}[\text{Ox}] + k_{1}k_{3}k_{4}k_{5}k_{6}[\text{Cu}][\text{N}^{-}]^{2}[\text{Ox}] + k_{1}k_{3}k_{4}k_{5}k_{6}[\text{Cu}][\text{N}^{-}]^{2}[\text{Ox}] + k_{1}k_{3}k_{4$$

Mechanism B

$$\frac{\text{d[P]}}{\text{dt}} = \frac{1}{\left(k_{-1}k_{3}k_{7}k_{8}k_{9}\text{[Cu][MeOH][X][Dx][base]} + k_{-1}k_{-2}k_{7}k_{8}k_{9}\text{[Cu][MeOH][X]}^{2}\text{[Ox]} + k_{1}k_{3}k_{7}k_{8}k_{9}\text{[Cu][MeOH][Ox][base]} + k_{1}k_{-2}k_{7}k_{8}k_{9}\text{[Cu][MeOH][X]}^{2}\text{[Cu][MeOH][X]}^{2}\text{[Cu][MeOH][X]}^{2}\text{[Dx]}^{2}\text{[Cu][MeOH][X]}^$$

	at high [Cu]	at high [sub]	at high [Cu] and high [sub]
A	$\frac{\text{d[P]}}{\text{dt}} = \frac{K_1 k_2 k_5 [\text{Pd}_T] [\text{sub}] [\text{MeOH}] [\text{base}]}{K_1 k_2 [\text{sub}] + k_5 [\text{MeOH}] ([\text{X}^-] + K_1)}$	$\frac{\text{d[P]}}{\text{dt}} = \frac{k_4 k_5 [\text{Pd}_T] [\text{Cu}] [\text{MeOH}] [\text{base}]}{k_4 [\text{Cu}] + k_5 [\text{MeOH}] [\text{base}] + k_{-4} [\text{X}^-]}$	$\frac{\text{d[P]}}{\text{dt}} = k_5 [\text{Pd}_{\text{T}}] [\text{MeOH}] [\text{base}]$
В	$\frac{\text{d[P]}}{\text{dt}} = \frac{K_1 k_2 k_5 [\text{Pd}_T] [\text{sub}] [\text{MeOH}] [\text{base}]}{K_1 k_2 [\text{sub}] + k_9 [\text{MeOH}] ([\text{X}^-] + K_1)}$	$\frac{d[P]}{dt} = \frac{k_7 k_9 [Pd_T][Cu][MeOH][base]}{k_9 [MeOH][base] + k_7 [Cu]}$	$\frac{d[P]}{dt} = k_9 [Pd_T] [MeOH] [base]$

Table 4

Hammett and Jaffé equations.

Hammett Equation:	Jaffé Equation:
$\log\left(\frac{k_{\rm X}}{k_{\rm H}}\right) = \rho_{\rm m}\sigma_{\rm m} + \rho_{\rm p}\sigma_{\rm p}$	$\frac{\log\left(\frac{k_{\mathrm{X}}}{k_{\mathrm{H}}}\right)}{\sigma_{\mathrm{m}}} = \frac{\rho_{\mathrm{p}}\sigma_{\mathrm{p}}}{\sigma_{\mathrm{m}}} + \rho_{\mathrm{m}} \text{ or } \frac{\log\left(\frac{k_{\mathrm{X}}}{k_{\mathrm{H}}}\right)}{\sigma_{\mathrm{p}}} = \frac{\rho_{\mathrm{m}}\sigma_{\mathrm{m}}}{\sigma_{\mathrm{p}}} + \rho_{\mathrm{p}}$

Table 5

Evaluation of copper complexes with achiral ligands.

4 mo% Pd((S)-quinox-IP1C)2

6 mol% Cu(ligand)Cl2

7 mol% (S)-quinox-IP1

C mol% (S)-quinox-IP1 40 mol% KHCO₃ 1:4 MeOH:toluene, O₂, rt

entry	copper complex	time	% conv.	% conv. % yield % ee	% ee	Ē
П	$\mathrm{Cu}(2,2$ '-bipyridine) Cl_2	30 min.	31	3	80	5:
		2 days	66	55	12	9:
2	Cu(phenanthroline)Cl ₂	30 min.	30	7	81	7:
		2 days	86	52	18	9:
33	$Cu(bathocuproine)Cl_2$	5 min.	27	6	91	9:
		10 min.	53	22	91	9:
		30 min.	98	49	92	9:
		2 h	100	63	91	7:
4	Pd(MeCN) ₂ Cl ₂ , CuCl ₂ 14 mol% bathocuproine	30 min.	19	1	;	9:
		2 h	50	5	;	5:
		17 h	96	27	;	13

Page 37

Jensen et al.

Page 38

Evaluation of Lewis acid additives.

4 mol% Pd(MeCN)₂Cl₂
8 mol% Lewis Acid
14 mol% (S)-quinox-IPr

ontar	ontary I omic offd	colvont	time	0/. conv	Ploix %		į
CHLL y	Lewis acid	30140111	TIIIT.	/0 COII.	o yren	5	3
1	-	1:1 THF:tol	19 h	43	2	pu	pu
2	CuCl	toluene	30 min	76	75	97:3	8:1
3	$CuCl_2$	1:1 THF:tol	30 min	100	81	97:3	11:1
4	$FeCl_3$	toluene	17 h	66	57	90:10	6:1
5	$FeCl_3$	1:1 THF:tol	19 h	62	22	92:8	4.5:1
9	$ZnCl_2$	toluene	17 h	29	9	94:6	4:1
7	$ZnCl_2$	1:1 THF:tol	19 h	77	28	95:5	4:1

Table 6

Jensen et al.

Page 39

Table 7

Evaluation of pyrox-tBu ligand derivatives.

	OH OWe	9
R = CF ₃ (17), CI (18), H (19), Me (20), OMe (21)	4 IIIO/8 FU(MECN/2C)2 8 mol% CuCl 14 mol% (S)-4-R-pyrox-fBu	40 mol% KHCO ₃ , 1:2:2 MeOH:tol:THF, O ₂ , π
	Б <u>-</u>	

entry	R	time	time % conv.	% yield % ee	% ee	er	dr
1	CF_3	3 h	29	46	6.89	84.5:15.5	15:1
2	IJ	3 h	29	39	74.2	87.1:12.9	13:1
33	Н	3 h	83	56	82.1	91.0:9.0	14:1
4	Me	3 h	79	49	81.6	90.8:9.2	13:1
5	OMe	3 h	79	49	81.7	90.9:9.1	14:1

Table 8

Enantiomeric ratio and diastereomeric ratio for product derivatives.

entry	R	ee (%)	er	dr
1	F	97.8	98.9:1.1	2.9:1
2	Cl	93.9	97.0:3.0	4.5:1
3	Н	93.2	96.6:3.4	8.1:1
4	Me	93.8	96.9:3.1	6.8:1
5	OMe	85.2	92.6:7.4	9.9:1